Plasma sheath and presheath development near a partially reflective surface

Boris N. Breizman [1] and Dmitrii I. Kiramov [1,2,†]

[1]Institute for Fusion Studies, The University of Texas, Austin, TX 78712, USA

[2]National Research Centre Kurchatov Institute, pl. Kurchatova 1, Moscow 123182, Russian Federation

This work addresses one-dimensional evolution of a collisionless plasma next to a solid surface that is immersed into the plasma instantaneously. In particular, we consider how the self-similar rarefaction wave (Allen & Andrews, *J. Plasma Phys.*, vol. 4, 1970, pp. 187–194) establishes dynamically and how the electron reflection from the surface modifies the structure of the rarefaction wave and the Debye sheath. We demonstrate that a sufficiently strong reflection eliminates the Debye sheath and changes the wall potential and the plasma flow parameters significantly. The paper presents numerical results that illustrate the developed analytical theory.

Key words: plasma sheaths, plasma nonlinear phenomena

---

1. Introduction

The problem of sheath formation at the plasma boundary is one of the oldest in plasma physics (Tonks & Langmuir 1929; Bohm 1949). It, nevertheless, still attracts considerable attention and reveals new twists (Campanell & Umansky 2016). The conventional set-up is for a finite or semi-infinite plasma region (see, e.g., reviews by Riemann 1991, 2008; Franklin 2003). In applications, the boundary of this region can be a probe's surface (Hutchinson 2002), a divertor plate (Stangeby 2000) or an anode of a discharge tube (Lieberman & Lichtenberg 1994). We further call this boundary a wall. The plasma electrons can charge the wall surface rapidly with plasma ions remaining virtually immobile in the process. A negative potential will thus build up at the wall long before the ion motion begins. This potential lowers the electron flux to the wall and attracts the ions. The wall potential eventually establishes a balance between the electron and ion fluxes. A sheath forms near the wall as a result with a positive space charge within several Debye lengths λ_D.

This simple picture, however, veils an issue that was initially highlighted by Bohm (see Bohm 1949): a stationary sheath exists only if the ions enter the sheath with a finite velocity equal to or greater than the ion sound speed (Stangeby & Allen 1970). This implies that there is a plasma region (presheath) where the ions accelerate. The presheath width L can depend on the ion mean free path, the ionization length, or the geometry of the system. The boundary plasma models (Riemann 1991) typically involve a scale separation

† Email address for correspondence: dmitrii.kiramov@austin.utexas.edu

between the sheath and the presheath: $L \gg \lambda_D$. It is then allowable to treat the sheath and the quasi-neutral presheath separately and match the solutions subsequently (Riemann *et al.* 2005). However, this approach often implies a steady flow and does not explain how the sheath and presheath form dynamically.

A dynamic problem arises when a solid object enters the plasma instantaneously. This problem is an essential part of the time-dependent probe theory (see, e.g., Widner *et al.* 1970). The initial state has neither sheath nor presheath. Over time the length scale separation establishes naturally as the presheath stretches from the sheath into the plasma bulk (Braithwaite & Wickens 1983). Allen & Andrews (1970) postulates the Bohm condition (Bohm 1949) in describing evolution of the presheath. In a later work (Cipolla & Silevitch 1981), the Bohm criterion for a time-dependent problem came out asymptotically in time as a result of the analysis so that the long-time behaviour of the presheath coincides with that of Allen & Andrews (1970).

In this paper, we present an explicit analytical solution to the transient problem of sheath formation. The constructed solution does not restrict the ions to have any particular initial velocity at the sheath–presheath interface, i.e. the initial ion velocity can be either subsonic or supersonic. In both cases, the Bohm criterion at the interface establishes asymptotically. The asymptotic behaviour of the presented solution matches that of Allen & Andrews (1970) and Cipolla & Silevitch (1981). We then generalize the results of Allen & Andrews (1970) and Cipolla & Silevitch (1981) by considering electron reflection from the wall. We show that, in the limit of strong reflection, the sheath weakens, and the ion flow differs significantly from that predicted in Allen & Andrews (1970) and Cipolla & Silevitch (1981).

2. Basic equations

We consider a one-dimensional plasma half-space ($x > 0$) in contact with a solid wall at $x = 0$. The ions are cold and initially immobile, and the electrons are initially Maxwellian. The wall mimics the surface of a solid object placed abruptly into the plasma. We assume that the wall absorbs the incident plasma electrons with a probability ε and reflects them with a probability $p \equiv 1 - \varepsilon$. We consider a simple case of incomplete specular and energy-conserving electron reflection. Consequently, the wall charging rate vanishes when $p = 1$ and is maximal at $p = 0$. This assumption presents a significant simplification of the actual electron reflection process, which indeed cannot be parameterized by a single parameter p. However, we believe that this idealization is adequate to illustrate the effect of electron reflection on the plasma sheath and presheath and to highlight the robust trend for sheath weakening. We also assume that there is no secondary electron emission from the wall. This implies that the wall temperature and the wall potential are significantly lower than the work function of the wall material.

The negative surface charge at the wall and the related electrostatic potential control the electron flux. The bulk electrons need to overcome the wall potential to reach the wall surface. The ion flux to the wall becomes significant only after several ion plasma periods $\omega_{pi}^{-1} = \sqrt{M/(4\pi n_\infty e^2)}$, where n_∞ is the ambient plasma density, $|e|$ is the unit charge and M is the ion mass. Over this timescale, the electron flux to the wall can already build a repelling potential that admits only the high-energy tail of the electron distribution to the wall surface. After that, the density of the flux-carrying tail electrons is a small fraction of the total electron density. Most electrons (the thermal electron bulk) do not reach the wall and remain quasi-static for $t \gg \omega_{pi}^{-1}$ with their density determined by the Boltzmann formula. Note that electron reflection from the wall itself also facilitates the use of the Boltzmann expression.

In the transient problem of sheath formation, the ions are immobile at $t = 0$ everywhere throughout the system, and they remain immobile at the spatial infinity at any time. The ion flow in this system starts near the wall and spreads into the unperturbed plasma. We herein neglect the ion thermal motion and use fluid equations to describe the ion flow:

$$\frac{\partial n}{\partial \tau} + \frac{\partial}{\partial \xi}(nu) = 0, \tag{2.1}$$

$$\frac{\partial u}{\partial \tau} + u \frac{\partial}{\partial \xi} u = \frac{\partial \psi}{\partial \xi}, \tag{2.2}$$

where n is the ion density (normalized to n_∞), u is the ion velocity (normalized to $\sqrt{T_e/M}$), $\tau = t\omega_{\mathrm{pi}} \geqslant 0$ is the normalized time, $\xi = x/\lambda_D$ is the space coordinate measured in the units of the Debye length $\lambda_D = \sqrt{T_e/(4\pi n_\infty e^2)}$ and T_e is the constant electron temperature. The normalized electrostatic potential $\psi = -|e|\varphi/T_e$ satisfies the Poisson equation,

$$\frac{\partial^2 \psi}{\partial \xi^2} = n - \exp(-\psi), \tag{2.3}$$

with the Boltzmann expression for the electron density. We assume that the electrostatic potential vanishes at infinity. A difference between the electron and the ion fluxes to the wall determines how the electric field builds up at $\xi = 0$:

$$\frac{\mathrm{d}}{\mathrm{d}\tau} \frac{\partial \psi}{\partial \xi} = -nu - \Delta \exp(-\psi). \tag{2.4}$$

The two terms on the right-hand side of (2.4) are the ion and the electron fluxes, respectively, at $\xi = 0$, $\Delta = \varepsilon \sqrt{M/(2\pi m)}$ is the normalized electron absorption probability and m is the electron mass. There are two additional conditions for (2.1)–(2.3).

(i) The plasma remains unperturbed far away from the wall, i.e.

$$n(\xi \to \infty, \tau) = 1, \quad u(\xi \to \infty, \tau) = 0, \quad \frac{\partial \psi}{\partial \xi}(\xi \to \infty, \tau) = 0. \tag{2.5a–c}$$

(ii) The plasma is unperturbed initially:

$$n(\xi, \tau = 0) = 1, \quad u(\xi, \tau = 0) = 0, \quad \psi(\xi, \tau = 0) = 0. \tag{2.6a–c}$$

In a steady state, equation (2.4) determines a floating potential ψ_0 that balances the ion and the electron fluxes,

$$\psi_0 = -\ln[n_0 |u_0|] + \ln \Delta, \tag{2.7}$$

where n_0 and u_0 are the ion density and the ion velocity at the wall, respectively.

The initial condition (2.6a–c) means that the solid wall is introduced instantaneously at $\tau = 0$ and $\xi = 0$, which would generally require to resolve an extremely short electron timescale, $\omega_{\mathrm{pe}}^{-1} = \sqrt{m/M}\omega_{\mathrm{pi}}^{-1}$. This timescale is already sufficient to accumulate a significant negative charge on the surface unless the wall is strongly reflective (see §7). The electron distribution deviates substantially from the Maxwellian during this short time, and, as already indicated in Cipolla & Silevitch (1981), the electrons must be treated kinetically. It is, however, appropriate to use the Boltzmann distribution in (2.3) and (2.4) on the ion timescale of our interest when the electron flux to the wall is

already small. The initial ($t \sim \omega_{\mathrm{pe}}^{-1}$) inconsistency caused by the unjustified Boltzmann assumption becomes asymptotically insignificant (see also Cipolla & Silevitch 1981). Keeping this remark in mind, we use (2.6*a*–*c*) in our numerical studies to describe the long-time evolution of the system. Our analytical studies also ignore this inconsistency, except for the linear theory in § 7 that does not require such a caveat.

3. A quasi-stationary sheath

The ion time of flight through the Debye sheath near the wall is roughly $\omega_{\mathrm{pi}}^{-1}$. A sheath that evolves on a much longer timescale can thus be viewed as quasi-stationary. The long timescale of our interest here characterizes propagation of the rarefaction wave from the sheath into the unperturbed plasma. In this case, one can neglect the time derivatives in the ion equation of motion (2.2) and the continuity equation (2.1) and integrate them over ξ to find the ion energy and the ion flux in the sheath:

$$
\left.
\begin{aligned}
nu &= n_b u_b, \\
\frac{u^2}{2} - \psi &= \frac{u_b^2}{2} - \psi_b,
\end{aligned}
\right\}
\tag{3.1}
$$

where $\psi_b(\tau)$, $n_b(\tau)$ and $u_b(\tau)$ are the values of ψ, n and u at an interface between the sheath and the adjacent rarefaction wave. With (2.3) and (3.1), we obtain the well-known (see, e.g., Bellan 2008) equation:

$$
\frac{\partial^2 \psi}{\partial \xi^2} = n_b \left(1 + \frac{2 \left(\psi - \psi_b \right)}{u_b^2} \right)^{-1/2} - \exp \left(-\psi \right).
\tag{3.2}
$$

Integration of (3.2) over ξ twice gives the following implicit expression for the electrostatic potential:

$$
\int_\psi^{\psi_0(\tau)} \frac{\mathrm{d}\psi}{\sqrt{D \left(\psi, \tau \right)}} = \xi,
\tag{3.3}
$$

where

$$
\begin{aligned}
\frac{1}{2} D \left(\psi, \tau \right) = {}&\frac{1}{2} \left(\frac{\partial \psi_b}{\partial \xi} \right)^2 + n_b u_b^2 \left[\left(1 + \frac{2 \left(\psi - \psi_b \right)}{u_b^2} \right)^{1/2} - 1 \right] \\
&+ \left[\exp \left(-\psi \right) - \exp \left(-\psi_b \right) \right],
\end{aligned}
\tag{3.4}
$$

and ψ_0 is the electrostatic potential at the surface of the wall. Note that (3.3) determines the sheath width $\ell(\tau)$ as a function of time:

$$
\ell \left(\tau \right) = \int_{\psi_b(\tau)}^{\psi_0(\tau)} \frac{\mathrm{d}\psi}{\sqrt{D \left(\psi, \tau \right)}}.
\tag{3.5}
$$

The ion velocity u_b, the ion density n_b, the electrostatic potential ψ_b and the electric field $\partial \psi_b / \partial \xi$ at the interface need to match their values in the rarefaction wave that we describe next.

4. The rarefaction wave

Once placed into the plasma, the wall creates a wave that propagates outward. The perturbed region between the wall and the wavefront involves an ion flow toward the wall.

In this section, we consider such flow as a stand-alone building block. We assume that the length of the perturbed region exceeds the Debye length substantially. In this case, the plasma must be quasi-neutral far away from the wall, which simplifies the Poisson equation (2.3) to

$$n = \exp(-\psi). \tag{4.1}$$

The flows of our interest connect the unperturbed immobile plasma to the wall and satisfy the following requirements:

   (i) the ion velocity, the electrostatic potential and density perturbations must all vanish far away from the wall;
  (ii) the wall acts as a plasma sink;
 (iii) the ultimate solution, of which the quasi-neutral flow is a part, must satisfy the boundary conditions at the wall.

It is important to point out that the quasi-neutral flow itself does not have to satisfy the boundary condition (2.4). It may, instead, match the sheath solution (3.1) and (3.3). In the spirit of Allen & Andrews (1970), we first consider the quasi-neutral flow adjacent to the quasi-static sheath.

To proceed further, we seek a particular solution of (2.1), (2.2) and (4.1) keeping in mind the listed requirements. To construct such solution, we use the following *ad hoc* expressions:

$$\left.\begin{aligned}
u &= u_1(\tau)\,(\xi - L(\tau)), \\
\psi &= -\psi_1(\tau)\,(\xi - L(\tau)),
\end{aligned}\right\} \tag{4.2}$$

where $L(\tau)$, $u_1(\tau)$ and $\psi_1(\tau)$ are yet unknown functions of time. The function $L(\tau)$ determines the interface between the rarefaction wave and the unperturbed plasma so that the velocity and the electrostatic potential vanish simultaneously at $\xi = L(\tau)$. Substitution of (4.1) and (4.2) into the system (2.1) and (2.2) gives the following solution for $u_1(\tau)$, $\psi_1(\tau)$ and $L(\tau)$:

$$\left.\begin{aligned}
\psi_1(\tau) = u_1(\tau) &= \frac{1}{\tau + \tau_*}, \\
L(\tau) &= L_* + \tau + \tau_*,
\end{aligned}\right\} \tag{4.3}$$

where τ_* and L_* are the integration constants. The resulting expressions for the ion velocity, the ion density and the electrostatic potential in the rarefaction wave are

$$\left.\begin{aligned}
u = -\psi &= \left(-1 + \frac{\xi - L_*}{\tau + \tau_*}\right)\theta\,(L_* - \xi + \tau + \tau_*), \\
n &= \exp\left[\left(-1 + \frac{\xi - L_*}{\tau + \tau_*}\right)\theta\,(L_* - \xi + \tau + \tau_*)\right],
\end{aligned}\right\} \tag{4.4}$$

where θ is the Heaviside step function and $\xi > 0$.

It turns out that the quasi-static sheath is not always required to match the quasi-neutral ion flow to the wall (see § 7 for further details). We also note that an interval of spatially uniform (ballistic) quasi-neutral flow between the wall and $L_-(\tau) < L(\tau)$ would satisfy (2.1), (2.2) and (4.1). The rarefaction wave (4.4) can be connected continuously to such

flow by choosing

$$\left.\begin{aligned}
L_-\left(\tau\right) &= L_* + \left(1 - \delta u\right)\left(\tau + \tau_*\right), \\
u &= -\psi = -\delta u\theta\left(L_-\left(\tau\right) - \xi\right), \\
n &= \exp\left[-\delta u\theta\left(L_-\left(\tau\right) - \xi\right)\right].
\end{aligned}\right\} \tag{4.5}$$

The boundary condition (2.4) can then determine a constant velocity $0 < \delta u < 1$ of the ballistic flow. In §§ 5–7, we discuss the matching procedure and the conditions under which either the quasi-static sheath or the ballistic flow can be established near the wall.

Except for the integration constants τ_* and L_*, equation (4.4) replicates the self-similar solution described in Allen & Andrews (1970) where all dependent variables were assumed to be functions of ξ/τ only. These two constants help to illustrate how the self-similar solution of Allen & Andrews (1970) establishes dynamically. Their values can, in principle, be found from a more general treatment of the quasi-neutral flow via the method of characteristics used in Cipolla & Silevitch (1981). However, to do that one needs a dynamical description of the sheath edge, which would necessarily involve numerical simulation of the sheath. On the other hand, the key features of the flow can already be understood from the rough physics constraints on τ_* and L_*, as discussed in § 5.

Equation (4.4) and Cipolla & Silevitch (1981) reveal that the Bohm condition $u \to 1$ establishes asymptotically in time at the edge of the sheath. In this case, the sheath edge is not necessarily immobile but rather moves slowly (see § 5).

Note that the electric field is spatially uniform within the rarefaction wave (4.4) and has a jump at the leading edge of the wave where $\xi = L(\tau)$

$$\frac{\partial\psi}{\partial\xi} = -\frac{1}{\tau + \tau_*}\theta\left(L_* - \xi + \tau + \tau_*\right). \tag{4.6}$$

Consequently, there is a surface charge at the leading edge, i.e. the quasi-neutrality condition (4.1) breaks down around the edge. However, the dispersive corrections regularize this weak discontinuity in a way discussed in Gurevich & Pitaevskii (1975).

5. Sheath-dominated reflection

To match the sheath and the rarefaction wave, we have to specify the unknown constants L_* and τ_* (see (4.4)). These constants are the only free parameters in our model. Note that we treat the problem separately in the sheath and the outside region. This procedure is justified when $L(\tau)$ is much greater than the sheath width $\ell(\tau)$. Up until that point, the two regions are inseparable, which precludes simple matching. The constants L_* and τ_* need to be chosen accordingly.

The constants L_* and τ_* determine the initial ($\tau = 0$) profiles of the plasma density, velocity and electrostatic potential. As seen from (4.3) and (4.4), the initial presheath length is $L_* + \tau_*$, and the initial ion velocity at the sheath–presheath interface is $-1 - L_*/\tau_*$. Since we treat the sheath and the presheath separately for any τ (including $\tau = 0$), the initial presheath length must be greater than unity ($L_* + \tau_* \gg 1$). The initial ion velocity at the interface can generally differ from -1 significantly. Different values of the L_*/τ_* ratio for $L_* + \tau_* \gg 1$ give a set of possible initial two-scale plasma profiles for (3.1), (3.3) and (4.4). In our problem, the constants L_* and τ_* carry memory about the short transient stage during which all the length scales are of order unity. The ion velocity at the wall can, in principle, be either subsonic or supersonic in the transient regime because the L_*/τ_* ratio is not necessarily positive. Our (3.1), (3.3) and (4.4) with $L_* + \tau_* \gg 1$ and $-1 - L_*/\tau_* < 0$ generalize the results of Cipolla & Silevitch (1981) and Allen & Andrews (1970) while keeping the correct asymptotic behaviour first predicted in

Allen & Andrews ([1970](#)). The self-similar solution of Allen & Andrews ([1970](#)) is recovered in the limit of $\tau \to \infty$, or by simply setting $L_* = \tau_* = 0$ in ([4.4](#)). This asymptotic solution describes the actual ion flow to the lowest order in λ_D/L.

On the other hand, the key features of the flow can be assessed without exact knowledge of τ_* and L_*. Equation ([4.4](#)) suggests that the velocity at the interface between the sheath and the rarefaction wave $[\xi = \ell(\tau) \ll L(\tau)]$ is $u_b(\tau) = -1 - L_*/(\tau + \tau_*)$ whereas the extension of the rarefaction wave is $L(\tau) = L_* + \tau + \tau_*$. Let us first assume that the velocity at the sheath-wave boundary exceeds the ion sound speed at some instant, i.e. $L_*/(\tau + \tau_*) > 0$. In this case, $u_b(\tau)$ stays supersonic afterwards and approaches the Bohm's limit from above asymptotically. By matching the sheath ([3.1](#)), ([3.3](#)) and the rarefaction wave ([4.4](#)) solutions, we find the following asymptotic behaviour of the wall potential in this case:

$$\psi_0(\tau) = \psi_0(\infty) + \frac{1}{2}\frac{L_*^2}{(\tau + \tau_*)^2}, \tag{5.1}$$

where $\psi_0(\infty) = 1 + \ln \Delta$ is the constant floating potential with $\Delta > 1$. The corresponding estimate for $\ell(\tau)$ from ([3.5](#)) is

$$\ell(\tau) = \sqrt{\frac{\exp(1)}{2|L_*|}}\sqrt{\tau + \tau_*}\ln\sqrt{\tau + \tau_*}, \tag{5.2}$$

We note that the ratio $\ell(\tau)/L(\tau)$ asymptotically vanishes as $\tau \to \infty$. This is consistent with a scale separation assumed in §§ [3](#)–[5](#).

As follows from ([4.4](#)), the ion velocity at the boundary between the sheath and the rarefaction wave approaches the ion sound speed at $\tau \to \infty$. It is, however, interesting that this approach can be either monotonic or oscillatory in space, depending on whether the instantaneous velocity is supersonic or subsonic. To examine this feature, we set $\psi = \psi_b(\tau) + \delta\psi$ and expand the Poisson equation ([3.2](#)) in $\delta\psi$ in the vicinity of the interface between the sheath and the rarefaction wave. We then obtain

$$\frac{\partial^2 \delta\psi}{\partial \xi^2} - \left[\exp(-\psi_b) - \frac{n_b}{u_b}\right]\delta\psi = n_b - \exp(-\psi_b). \tag{5.3}$$

The right-hand side of this equation vanishes because of the quasi-neutrality condition ([4.1](#)), which reduces ([5.3](#)) to

$$\frac{\partial^2 \delta\psi}{\partial \xi^2} - \frac{n_b}{u_b^2}\left(u_b^2 - 1\right)\delta\psi = 0. \tag{5.4}$$

Note that ([5.4](#)), reminiscent of the Bohm's analysis, describes spatial oscillations of the electrostatic potential around its boundary value $\psi_b(\tau)$ in the subsonic case ($|u_b| < 1$) as opposed to an exponential profile in the supersonic case ($|u_b| > 1$). In the conventional stationary sheath models (see, e.g., Riemann [1991](#)), the oscillatory solutions are considered unphysical because of a strong potential variation of order unity in the presheath contradicting the assumed length scale ordering. However, these oscillations are meaningful in the dynamics. They do occur transiently, but their spatial scale $\ell_\sim^{-2}(\tau) \equiv n_b(u_b^2 - 1)/u_b^2$ (determined by the coefficient in front of $\delta\psi$ in ([5.4](#))) grows in time. Indeed, with ([4.4](#)), one finds that $\ell_\sim \propto (\tau + \tau_*)^{1/2}$ at $\tau \to \infty$ so that the oscillations eventually smooth out. It is important to point out that our model does not resolve the short initial time interval during which the sheath forms and the rarefaction wave establishes.
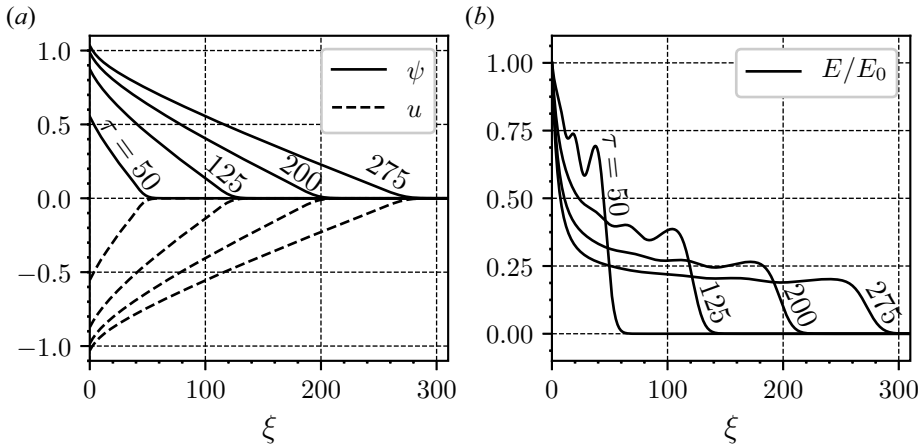
FIGURE 1. Numerical solution of (2.1)–(2.3). The normalized electric field $E = \partial\psi/\partial\xi$ at the surface of the wall is fixed in this case to be $E_0 = -0.015$. (*a*) Snapshots of the electrostatic potential (solid lines) and the ion velocity (dashed lines) for several times. (*b*) Snapshots of the electric field normalized to its constant value at the surface of the wall E_0.

Owing to this, the initial ion velocity at the interface between the sheath and the rarefaction wave enters as an input parameter $u_b(0) = -1 - L_*/\tau_*$. If the ratio L_*/τ_* is negative and small, i.e. the initial velocity is slightly subsonic, then the length scale of the oscillations can be much greater than unity. In this case, the oscillations near the merging point are virtually irrelevant. On the other hand, if L_*/τ_* is still negative but $|L_*/\tau_*| \sim 1$, the oscillations can stay pronounced over long time. To find out which of the two cases is more relevant for the system (2.1)–(2.3), one has to resolve the short initial phase, during which the electrostatic sheath forms and the length-scale separation establishes. It is straightforward to resolve this phase by integrating equations (2.1)–(2.3) numerically using a scheme similar to (Widner *et al.* 1970). Our numerical solution of (2.1)–(2.3) with the boundary condition given by (2.4) (and $\Delta > 1$) shows fast establishment of the floating potential (2.7) at the wall. The ion velocity at the sheath–wave interface is either slightly supersonic or slightly subsonic by the end of the initial stage in this case. This makes the rapidly decaying oscillations virtually unnoticeable. A boundary condition different from (2.4) would result in a different initial stage and highlight the otherwise negligible oscillations. To illustrate that and exhibit the oscillations, we artificially fix a small but finite value of the electric field at the wall and plot the resulting snapshots of the electrostatic potential, ion velocity and electric field in figure 1.

Figure 1(*b*) shows small spatial oscillations of the electric field at early times. The amplitude of these oscillations decreases over time, while their period increases. Figure 1(*a*) shows that the ion velocity at the wall approaches unity as the oscillations decay.

6. Sheath disappearance

The two-scale solution (3.3), (4.4) with a sheath breaks down when the wall is strongly reflective. To demonstrate that, we consider the charge balance condition (2.4) in the limit of large τ, assuming that the potential ψ is static in the sheath so that the time derivative vanishes on the left-hand side of (2.4). Equation (4.4), Allen & Andrews (1970) and Cipolla & Silevitch (1981) show that the normalized ion flux in the sheath

is $nu = -\exp(-1)$ at $\tau \to \infty$, which reduces (2.4) to

$$\exp(-1) = \Delta \exp(-\psi_0),\tag{6.1}$$

where ψ_0 is the wall potential.

On the other hand, the electrostatic potential at the interface between the sheath and the rarefaction wave approaches unity (see (4.4)) and the potential is monotonic in the sheath, which means that

$$\psi_0 \geqslant 1,\tag{6.2}$$

at $\tau \to \infty$. Equations (6.1) and (6.2) are obviously incompatible when Δ is less than unity. Consequently, the asymptotic sheath solution (3.3) and (4.4) fails and needs to be revised at $\Delta < 1$, i.e. in the case of strongly reflective wall.

It is unlikely that the case of $\Delta < 1$ is representative from an experimental standpoint because it implies an extremely small value of the absorption coefficient ε. Yet, this case is of theoretical interest as a caveat that the sheath not just weakens when ε is much smaller than unity but may altogether disappear. Consequently, calculation of the wall potential becomes non-trivial at $\varepsilon \ll 1$ in general, not just at $\varepsilon < \sqrt{2\pi m/M}$. Near the critical point $\Delta = 1$, a marginal change of the absorption coefficient, as we will show, radically changes the global structure of the flow: (i) the sheath does not form; (ii) the ions never reach the sound speed; and (iii) the rarefaction wave involves a ballistic flow (4.5) between the wall and the leading part of the wave (4.4). In the case of $\Delta < 1$, the resulting wall potential is proportional to Δ. It vanishes for a perfectly reflective wall ($\Delta = 0$) because the plasma is then at rest. If Δ exceeds unity by a small margin, i.e. $\Delta = 1 + \delta$ with $0 < \delta \ll 1$, the sheath solution is still applicable and the wall potential approaches unity when δ goes to zero.

To infer the listed results, we solve (2.1)–(2.3) with the boundary condition (2.4) numerically for small positive and negative values of δ and compare the snapshots of the electrostatic potential for large τ. Figure 2 reveals a transition from a small electrostatic sheath near the wall (dashed curve) to the flat near-wall potential (solid curve). The flat potential area represents the uniform ion flow to the wall. This flow connects to the leading part of the rarefaction wave in which there is a constant electric field (the potential has a constant slope). The rarefaction wave moves into the unperturbed plasma and leaves a uniform ballistic flow of accelerated ions behind. Note that the presence of the ballistic ion flow adjacent to the wall distinguishes the pattern from the conventional sheath model of Allen & Andrews (1970). In the conventional case, the rarefaction wave accelerates the ions to the sound speed, after which the sheath accelerates them further towards the wall. In contrast, the strongly reflective wall precludes accumulation of the negative surface charge and the sheath formation. Without a sheath, the ions remain subsonic and they come to the wall directly from the rarefaction wave. We discuss this scenario in more detail in § 7.

7. Wall-dominated reflection

We first assume that the entire ion flow is quasi-neutral and then generalize the picture to include deviations from quasi-neutrality in the flow. The quasi-neutral ballistic ion flow to the wall is subsonic and can be described by (4.5). Taken together, the quasi-neutrality condition (4.1) and (2.7) determine the ion velocity at the wall:

$$u_0 = -\Delta.\tag{7.1}$$

This velocity must match the self-similar solution (4.4) at a moving matching point $\xi = L_-(\tau)$, which determines the plasma density and the electrostatic potential drop across the
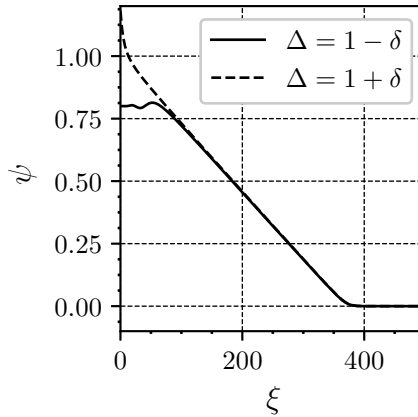
FIGURE 2. Numerical solution of (2.1)–(2.3). Snapshots of the electrostatic potential for $\Delta = 1 - \delta$ (solid line) and $\Delta = 1 + \delta$ (dashed line) at $\tau = 375$, where $\delta = 0.2$.

rarefaction wave (see also Landau & Lifshitz 1954):

$$n_0 = \exp(-\Delta), \left.\begin{array}{c} \\ \\ \end{array}\right\} \tag{7.2}$$
$$\psi_0 = \Delta.$$

The leading edge of the rarefaction wave travels into the unperturbed plasma with the sound speed, whereas the connection point $L_-(\tau) \sim (1 - \Delta)\tau$ moves forward with a lower speed so that both parts of the flow expand linearly with time. Equations (4.4) and (4.5) can now be conveniently combined into

$$u = -\psi = -\Delta \left[\theta(\xi/\tau) - \theta(\xi/\tau - 1 + \Delta)\right],$$
$$+ (\xi/\tau - 1)\left[\theta(\xi/\tau - 1 + \Delta) - \theta(\xi/\tau - 1)\right], \tag{7.3}$$

where $\xi > 0$ and $\tau \gg 1$.

It is instructive to compare (7.3) with a numerical solution of (2.1)–(2.3) without enforcing quasi-neutrality. In solving (2.1)–(2.3), we use the dynamical boundary condition (2.4) instead of the simplified floating condition (2.7). Figure 3 presents the resulting snapshots of the electrostatic potential, ion velocity and ion density for two different values of the wall absorption probabilities. In both cases, there are three distinct regions in the snapshots: the static unperturbed plasma, the rarefaction wave with a constant electric field and the ballistic flow of the accelerated ions to the wall. The values of the potential, velocity and density across the rarefaction wave agree with the analytical predictions (7.1) and (7.2).

Comparing the left and right panels in figure 3, we note that the velocity of the connection point $\xi = L_-(\tau)$ of the rarefaction wave to the ballistic flow depends on the wall absorption probability. The predicted velocities of both $L_-(\tau)$ and $L(\tau)$ (see (7.3)) agree with their numerical estimates (see figure 4).

Still, the quasi-neutral solution does not capture the small oscillations of density, potential and velocity behind the rarefaction wave. These oscillations result from the discontinuity of the profile slope in the quasi-neutral solution (see Gurevich & Meshcherkin 1984). Their amplitude decreases in time (Gurevich & Meshcherkin 1984) as the region they occupy expands. In contrast, the slope discontinuity at the leading edge of the rarefaction wave does not produce any oscillatory motion in its vicinity. There is
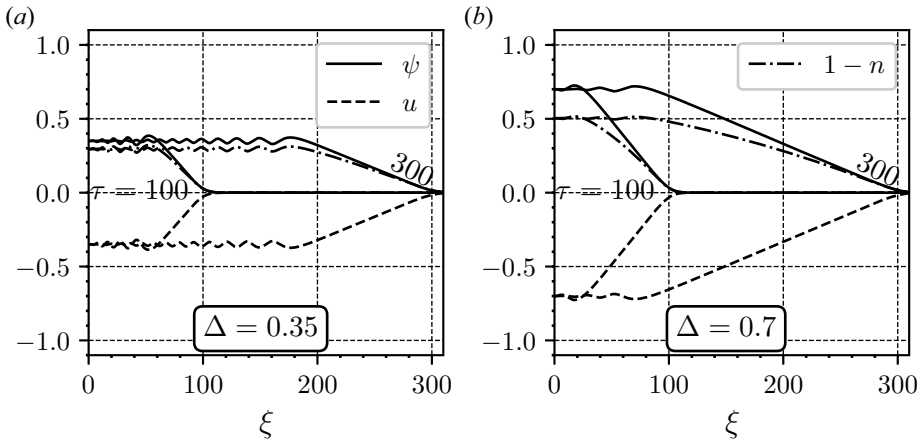
FIGURE 3. Numerical solution of (2.1)–(2.3) for a strongly reflective wall. (*a,b*) Snapshots of the electrostatic potential (solid lines), the ion velocity (dashed lines) and one minus the ion density (dash-dotted line) for several times. The normalized wall absorption probability Δ is marked in each panel.
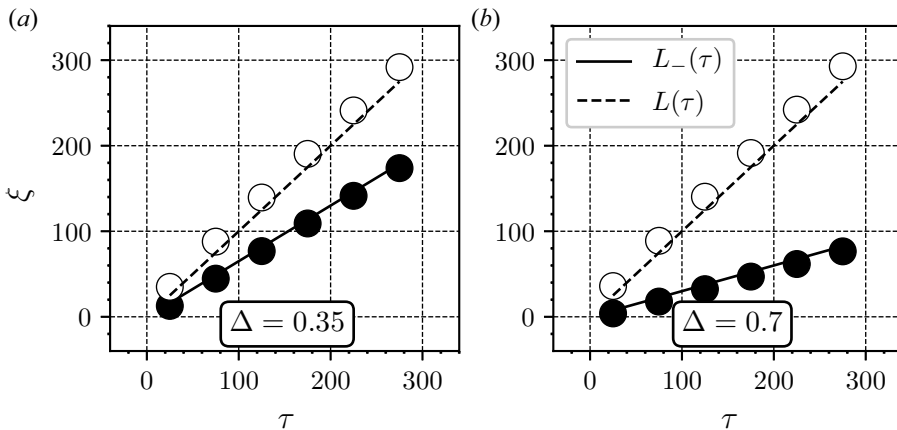
FIGURE 4. Time traces of the left (solid line and discs) and right (dashed line and circles) boundaries of the rarefaction wave. The solid and dashed lines in each panel represent our analytical solution (see (7.3)), dots and circles represent the corresponding numerical estimate (see also figure 3). The normalized wall absorption probability Δ is marked at the bottom of each panel.

an essential difference between the discontinuities at $L_-(\tau)$ and $L(\tau)$. The leading edge moves into the unperturbed plasma with the sound velocity. Consequently, it does not have a precursor. On the other hand, the ions that leave the wave at $L_-(\tau)$ can carry the perturbation into the ballistic flow.

The oscillatory nature of the solution is most evident in the limit of $\Delta \ll 1$, in which case it is allowable to linearize (2.1)–(2.3) while keeping the dispersive corrections in the equations. Note that the case of $\Delta \ll 1$ implies an extremely low (and possibly unrealistically low) absorption coefficient. Note also that additional factors such as, for instance, the finite ion temperature T_i (Emmert *et al.* 1980) or the secondary electron emission (Campanell & Umansky 2016) are likely to enter the game in the case

of $\Delta \sim T_i/T_e$. However, these factors are unlikely to change the dispersive features of the solution that we will highlight, although they deserve an independent assessment, which is beyond the limited scope of our paper. We then obtain the following linear equation for the electrostatic potential

$$\frac{\partial^2 \psi}{\partial \xi^2} - \psi = -\int_0^\tau \int_0^s \frac{\partial^2 \psi}{\partial \xi^2} (\xi, \sigma) \, d\sigma \, ds. \tag{7.4}$$

The linearized condition (2.4) for this equation is

$$\frac{d}{d\tau} \frac{\partial \psi}{\partial \xi} = -u - \Delta. \tag{7.5}$$

A straightforward Fourier transform of (7.4), and (7.5) returns the following solution for the electrostatic potential:

$$\psi = \Delta \frac{2}{\pi} \int_0^{+\infty} \frac{\cos k\xi}{\sqrt{1+k^2}} \sin \frac{k\tau}{\sqrt{1+k^2}} \frac{dk}{k}. \tag{7.6}$$

In particular, we find that the electrostatic potential, the electric field and the ion velocity at the wall ($\xi = 0$) are

$$\left.\begin{aligned} \psi_0 (\tau) &= \Delta \int_0^\tau J_0 (s) \, ds, \\ \frac{\partial \psi}{\partial \xi} (0, \tau) &= -\Delta \sin \tau, \\ u_0 (\tau) &= -\Delta (1 - \cos \tau) . \end{aligned}\right\} \tag{7.7}$$

Appendix A provides a detailed derivation of (7.6) and (7.7). Note that the wall potential oscillates, but the amplitude of these oscillations decays, and the potential asymptotically converges to $\langle \psi_0 \rangle = \Delta$. The plasma velocity at the wall and the electric field at the wall also oscillate but without any decay. The average values of the linearized plasma parameters correspond to their nonlinear dispersionless estimates (see (7.1) and (7.2)).

Figure 5 presents the linearized electrostatic potential as a function of ξ for $\tau = 50$ and $\tau = 500$. We observe that the linearized treatment does indeed capture the oscillatory behaviour of the nonlinear solution (see figure 3). Both boundaries of the rarefaction wave move with the sound speed in the linearized case. The wave front, therefore, does not broaden over time as opposed to the nonlinear case (compare figures 3 and 5).

8. Floating potential

The analysis presented in §§ 5–7 reveals an interesting aspect in the dependence of the wall potential on reflective properties of the wall. In the case of $\Delta > 1$, the asymptotic value of the potential at $\tau \to \infty$ depends logarithmically on the normalized wall absorption coefficient Δ (see (5.1)). On the other hand, in the case of $\Delta < 1$, the potential does not follow (5.1) anymore. Its dependence changes from the logarithmic to linear (see (7.2) and (7.7)). We, thus, have

$$\psi_0 = \begin{cases} 1 + \ln \Delta, & \text{if } \Delta > 1, \\ \Delta, & \text{if } \Delta \leqslant 1. \end{cases} \tag{8.1}$$

It is noteworthy that the transition is smooth in (8.1) as well as in our numerical results.

(*a*)

(*b*)
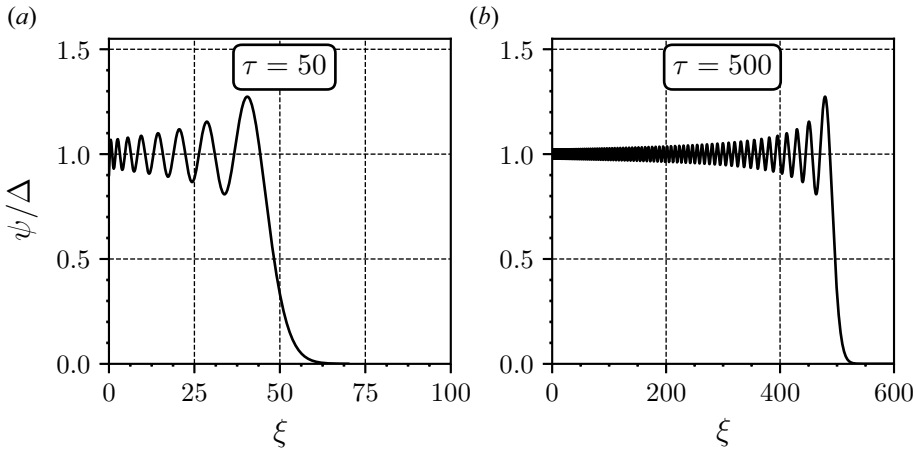
FIGURE 5. Snapshots of the linearized electrostatic potential (see (7.6)) normalized to the asymptotic wall potential $\langle \psi_0 \rangle = \Delta$ for (*a*) $\tau = 50$ and (*b*) $\tau = 500$.
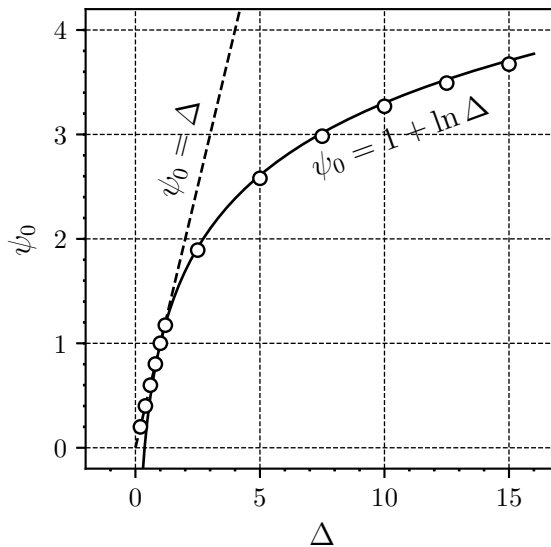
FIGURE 6. The floating potential as a function of the normalized wall absorption probability $\Delta = \varepsilon \sqrt{M/(2\pi m)}$. The solid and dashed curves represent the analytical expression (8.1). The circles show the time-averaged electrostatic potential of the wall in numerical simulations.

9. Summary

This paper generalizes the pre-existing one-dimensional analysis (Allen & Andrews 1970; Cipolla & Silevitch 1981) of collisionless plasma flow to the sold surface. Our analysis covers an intermediate evolution of the system, which takes place after fast formation of the electrostatic sheath and the rarefaction wave and precedes the asymptotic self-similar flow of Allen & Andrews (1970). The generalized solution is given by (3.1), (3.3) and (4.4). The only input parameters in this solution are the initial extension of the rarefaction wave and the initial ion velocity at the interface between the sheath and the rarefaction wave. Equation (4.4) of the generalized solution describes how the Bohm

criterion establishes asymptotically for both subsonic and supersonic initial velocities at the sheath entrance. The long-time evolution of the plasma flow coincides with that of Allen & Andrews (1970).

This paper also highlights the effect of electron reflection from the wall on the electrostatic sheath formation. We find that a sufficiently strong reflection from the wall precludes formation of the electrostatic sheath at the surface and makes the entire ion flow subsonic. We characterize the role of reflection by a dimensional parameter $\Delta = \varepsilon \sqrt{M/(2\pi m)}$ and determine a critical point ($\Delta = 1$) at which a slight change of the absorption coefficient changes the global structure of the flow significantly: the electrostatic sheath disappears, the rarefaction wave detaches from the wall and a region of ballistic flow near the wall emerges. The wall potential, in this case, exhibits an interesting transition in its dependence on the wall reflectivity (as described by (8.1) and shown in figure 6).

Acknowledgements

Editor Peter Catto thanks the referees for their advice in evaluating this article.

Declaration of interests

The authors report no conflict of interest.

Appendix A

This appendix provides a detailed derivation of (7.6) and (7.7). We first linearize (2.1)–(2.3) and the boundary condition (2.4) to obtain

$$
\left.\begin{aligned}
\frac{\partial n}{\partial \tau} + \frac{\partial u}{\partial \xi} &= 0, \\
\frac{\partial u}{\partial \tau} - \frac{\partial \psi}{\partial \xi} &= 0, \\
\frac{\partial^2 \psi}{\partial \xi^2} - \psi &= n,
\end{aligned}\right\}
\tag{A 1}
$$

and

$$
\frac{\mathrm{d}}{\mathrm{d}\tau} \left.\frac{\partial \psi}{\partial \xi}\right|_{\xi=+0} = -u\,(+0, \tau) - \Delta,
\tag{A 2}
$$

where n is the perturbed density. Equations (A 1) and (A 2) refer to positive values of ξ, i.e. to ($0 < \xi < \infty$), but it is convenient to extend the ξ-domain from $-\infty$ to $+\infty$. Note that (A 1) remains unchanged under parity $t, \xi, u \mapsto t, -\xi, -u$. Consequently, we treat n and ψ as even functions of ξ and u as an odd function. We also note that u and $\mathrm{d}\psi/\mathrm{d}\xi$ are generally discontinuous at $\xi = 0$. Taking this symmetry into account, we obtain the

following Fourier image of the system (A 1):

$$\left.\begin{aligned}
\frac{\mathrm{d}n_k}{\mathrm{d}\tau} + \mathrm{i}ku_k &= 2u\,(+0,\tau)\,, \\[4pt]
\frac{\mathrm{d}u_k}{\mathrm{d}\tau} - \mathrm{i}k\psi_k &= 0, \\[4pt]
\psi_k &= -\frac{n_k}{1+k^2} - \frac{2}{1+k^2}\left.\frac{\partial\psi}{\partial\xi}\right|_{\xi=+0},
\end{aligned}\right\} \tag{A 3}$$

where

$$\left.\begin{aligned}
n_k(\tau) &= 2\int_0^{+\infty} n(\xi,\tau)\cos k\xi\,\mathrm{d}\xi, \\[4pt]
\psi_k(\tau) &= 2\int_0^{+\infty} \psi(\xi,\tau)\cos k\xi\,\mathrm{d}\xi, \\[4pt]
u_k(\tau) &= -2\mathrm{i}\int_0^{+\infty} u(\xi,\tau)\sin k\xi\,\mathrm{d}\xi.
\end{aligned}\right\} \tag{A 4}$$

Equations (A 3) reduce to the following equation for the Fourier image of the perturbed density:

$$\frac{\mathrm{d}^2 n_k}{\mathrm{d}\tau^2} + \frac{k^2}{1+k^2}n_k = 2\frac{\mathrm{d}u}{\mathrm{d}\tau}(+0,\tau) - \frac{2k^2}{1+k^2}\left.\frac{\partial\psi}{\partial\xi}\right|_{\xi=+0}. \tag{A 5}$$

We next transform the right-hand side of (A 5). We use (A 1) and (A 2) evaluated at $\xi = +0$ to obtain

$$\frac{\mathrm{d}^2 u}{\mathrm{d}\tau^2}(+0,\tau) + u(+0,\tau) = -\Delta. \tag{A 6}$$

The electric field and the ion velocity at the wall are initially zero. We, therefore, obtain the following initial conditions from the second equation of (A 1):

$$\frac{\mathrm{d}u}{\mathrm{d}\tau}(+0,0) = u(+0,0) = 0. \tag{A 7}$$

We, thus, have

$$u(+0,\tau) = -\Delta\,(1-\cos\tau)\,. \tag{A 8}$$

Equation (A 8) and the boundary condition (A 2) determine the electric field at the wall:

$$\left.\frac{\partial\psi}{\partial\xi}\right|_{\xi=+0} = -\Delta\sin\tau. \tag{A 9}$$

We now use (A 8) and (A 9) to rewrite (A 5) as

$$\frac{\mathrm{d}^2 n_k}{\mathrm{d}\tau^2} + \frac{k^2}{1+k^2}n_k = -2\Delta\frac{\sin\tau}{1+k^2}. \tag{A 10}$$

We note that the ion density is not perturbed initially and use the first equation of (A 3) at $\tau = 0$ to impose the following initial conditions:

$$\frac{\mathrm{d}n_k}{\mathrm{d}\tau}(0) = n_k(0) = 0. \tag{A 11}$$

The resulting solution of (A 10) is

$$n_k = -2\Delta \frac{\sqrt{1+k^2}}{k} \sin \frac{k\tau}{\sqrt{1+k^2}} + 2\Delta \sin \tau. \tag{A 12}$$

The corresponding Fourier image of the electrostatic potential is (see (A 3))

$$\psi_k = \frac{1}{k} \frac{2\Delta}{\sqrt{1+k^2}} \sin \frac{k\tau}{\sqrt{1+k^2}}. \tag{A 13}$$

The inverse Fourier transform of (A 13) gives the electrostatic potential as a function of ξ and τ:

$$\psi(\xi, \tau) = \Delta \frac{2}{\pi} \int_0^{+\infty} \frac{\cos k\xi}{\sqrt{1+k^2}} \sin \frac{k\tau}{\sqrt{1+k^2}} \frac{\mathrm{d}k}{k}. \tag{A 14}$$

At the wall surface ($\xi = +0$), this expression simplifies to

$$\psi(+0, \tau) = \Delta \int_0^\tau J_0(s)\, \mathrm{d}s, \tag{A 15}$$

where $J_0(s)$ is the zeroth-order Bessel function of the first kind.

REFERENCES

ALLEN, J. E. & ANDREWS, J. G. 1970 A note on ion rarefaction waves. *J. Plasma Phys.* **4** (1), 187–194.
BELLAN, P. M. 2008 *Fundamentals of Plasma Physics*. Cambridge University Press.
BOHM, D. 1949 *The Characteristics of Electric Discharges in a Magnetic Field*, vol. 3. McGraw-Hill.
BRAITHWAITE, N. ST. J. & WICKENS, L. M. 1983 Plasma boundary motion and the ion-acoustic wave. *J. Plasma Phys.* **30** (1), 133–151.
CAMPANELL, M. D. & UMANSKY, M. V. 2016 Strongly emitting surfaces unable to float below plasma potential. *Phys. Rev. Lett.* **116**, 085003.
CIPOLLA, J. W. & SILEVITCH, M. B. 1981 On the temporal development of a plasma sheath. *J. Plasma Phys.* **25** (3), 373–389.
EMMERT, G. A., WIELAND, R. M., MENSE, A. T. & DAVIDSON, J. N. 1980 Electric sheath and presheath in a collisionless, finite ion temperature plasma. *Phys. Fluids* **23** (4), 803–812.
FRANKLIN, R. N. 2003 The plasma–sheath boundary region. *J. Phys. D: Appl. Phys.* **36** (22), R309–R320.
GUREVICH, A. V. & MESHCHERKIN, A. P. 1984 Expanding self-similar discontinuities and shock waves in dispersive hydrodynamics. *Zh. Eksp. Teor. Fiz.* **87**, 1277–1292.
GUREVICH, A. V. & PITAEVSKII, L. P. 1975 The structure of a weak discontinuity in dispersive hydrodynamics. In *Proceedings of the Twelfth International Conference on Phenomena in Ionized Gases, Eindhoven* (ed. J. G. A. Hoelscher & D. C. Schram), p. 273. North-Holland Publishing Company.
HUTCHINSON, I. H. 2002 *Principles of Plasma Diagnostics*, 2nd edn. Cambridge University Press.
LANDAU, L. D. & LIFSHITZ, E. M. 1954 *Mekhanika sploshnykh sred (Fluid Mechanics)*. Gostekhizdat.
LIEBERMAN, M. A. & LICHTENBERG, A. J. 1994 *Principles of Plasma Discharges and Materials Processing*. Wiley.
RIEMANN, K.-U. 1991 The Bohm criterion and sheath formation. *J. Phys. D: Appl. Phys.* **24** (4), 493–518.
RIEMANN, K.-U. 2008 Plasma and sheath. *Plasma Sources Sci. Technol.* **18** (1), 014006.
RIEMANN, K.-U., SEEBACHER, J., TSKHAKAYA, D. D. & KUHN, S. 2005 The plasma–sheath matching problem. *Plasma Phys. Control. Fusion* **47** (11), 1949–1970.
STANGEBY, P. C. & ALLEN, J. E. 1970 Plasma boundary as a Mach surface. *J. Phys. A: Gen. Phys.* **3** (3), 304.

STANGEBY, P. C. 2000 *The Plasma Boundary of Magnetic Fusion Devices*, vol. 224. Institute of Physics.

TONKS, L. & LANGMUIR, I. 1929 A general theory of the plasma of an arc. *Phys. Rev.* **34** (6), 876–922.

WIDNER, M., ALEXEFF, I., JONES, W. D. & LONNGREN, K. E. 1970 Ion acoustic wave excitation and ion sheath evolution. *Phys. Fluids* **13** (10), 2532–2540.